Micron 84 (2016) 54–60

Contents lists available at ScienceDirect

Micron

journal homepage: www.elsevier.com/locate/micron

3D scanning electron microscopy applied to surface characterization of fluorosed dental enamel

Silvina Limandri[a,b], Víctor Galván Josa[a,b], María Cecilia Valentinuzzi[a,b], María Emilia Chena[c], Gustavo Castellano[a,b,*]

[a] FaMAF, Universidad Nacional de Córdoba, Medina Allende s/n, Ciudad Universitaria, Córdoba, Argentina
[b] IFEG, CONICET, Medina Allende s/n, Ciudad Universitaria, Córdoba, Argentina
[c] Cátedra de Operatoria II A, Facultad de Odontología, UNC, Argentina

ARTICLE INFO

Article history:
Received 2 November 2015
Received in revised form 4 February 2016
Accepted 4 February 2016
Available online 20 February 2016

Keywords:
SEM
Stereomicroscopy
Surface topography
Functional and amplitude parameters
Fluorotic teeth

ABSTRACT

The enamel surfaces of fluorotic teeth were studied by scanning electron stereomicroscopy. Different whitening treatments were applied to 25 pieces to remove stains caused by fluorosis and their surfaces were characterized by stereomicroscopy in order to obtain functional and amplitude parameters. The topographic features resulting for each treatment were determined through these parameters. The results obtained show that the 3D reconstruction achieved from the SEM stereo pairs is a valuable potential alternative for the surface characterization of this kind of samples.

1. Introduction

Scanning electron microscopy (SEM) is a suitable technique to study materials surface characteristics. Although secondary electron images furnish apparent three-dimensional micrographs, information about local heights cannot be inferred straightforwardly from the gray levels in these images (Reimer, 1998).

Different approaches have been proposed in order to quantitatively recover the third dimension from SEM images (Tafti et al., 2015). One of the most investigated and popular methods for surface three-dimensional reconstruction is photogrammetry, also known as multiple-view approach, which is based in the acquisition of two stereo images (stereo pair) (Mohr and Wray, 1976). A theoretical description for SEM implementation was first provided by Piazzesi (1973), and the technique consists in the acquisition and subsequent processing of a series of images taken at different tilt angles (Schubert et al., 1996). The topographic reconstruction using two images is generally more used since only two steps are required. The stereo pairs can be acquired by tilting the sample, by tilting the electron beam or by using multiple detectors. The surface points can be identified relative to a reference point, and by considering the distances between them and their relative slopes; geometrical considerations allow to obtain the height distribution for the scanned region (Bonetto et al., 2006).

Quantitative height determinations at micro and nanometric scales are required in a variety of applications such as surface roughness determination (Bouacha et al., 2010), nanomaterials and nanodevices (Ferry et al., 2008), life sciences (Gittens et al., 2011; Choi et al., 2012; Kim, 2015), fracture analysis (Ficker et al., 2010), computer-vision (Harrison et al., 2011), and many others (Richards et al., 2000). In the particular case of dental whitening treatments analyzed in this work, it is essential to achieve surface roughness characteristics similar to those of a healthy tooth. Dental aesthetics is nowadays an important aspect in everyday life; much more important is the fact that changes in color of dental elements are the result of alterations in the tooth enamel. The enamel presents structural, physical and chemical characteristics whose knowledge is essential to understand their biological behavior, taking into account its important role in the mastication process (Avery, 1994).

Dental fluorosis can be caused by chronic ingestion of high levels of fluorine in water during tooth development (Vieira et al., 2004), or it may also originated in topical treatments with fluorine agents (Kohn et al., 2001). Despite fluorine being an important element to control dental caries, an excess of this element during dentin

* Corresponding author. Fax: +54 351 4334054.
E-mail address: gcas@famaf.unc.edu.ar (G. Castellano).

http://dx.doi.org/10.1016/j.micron.2016.02.001
0968-4328/

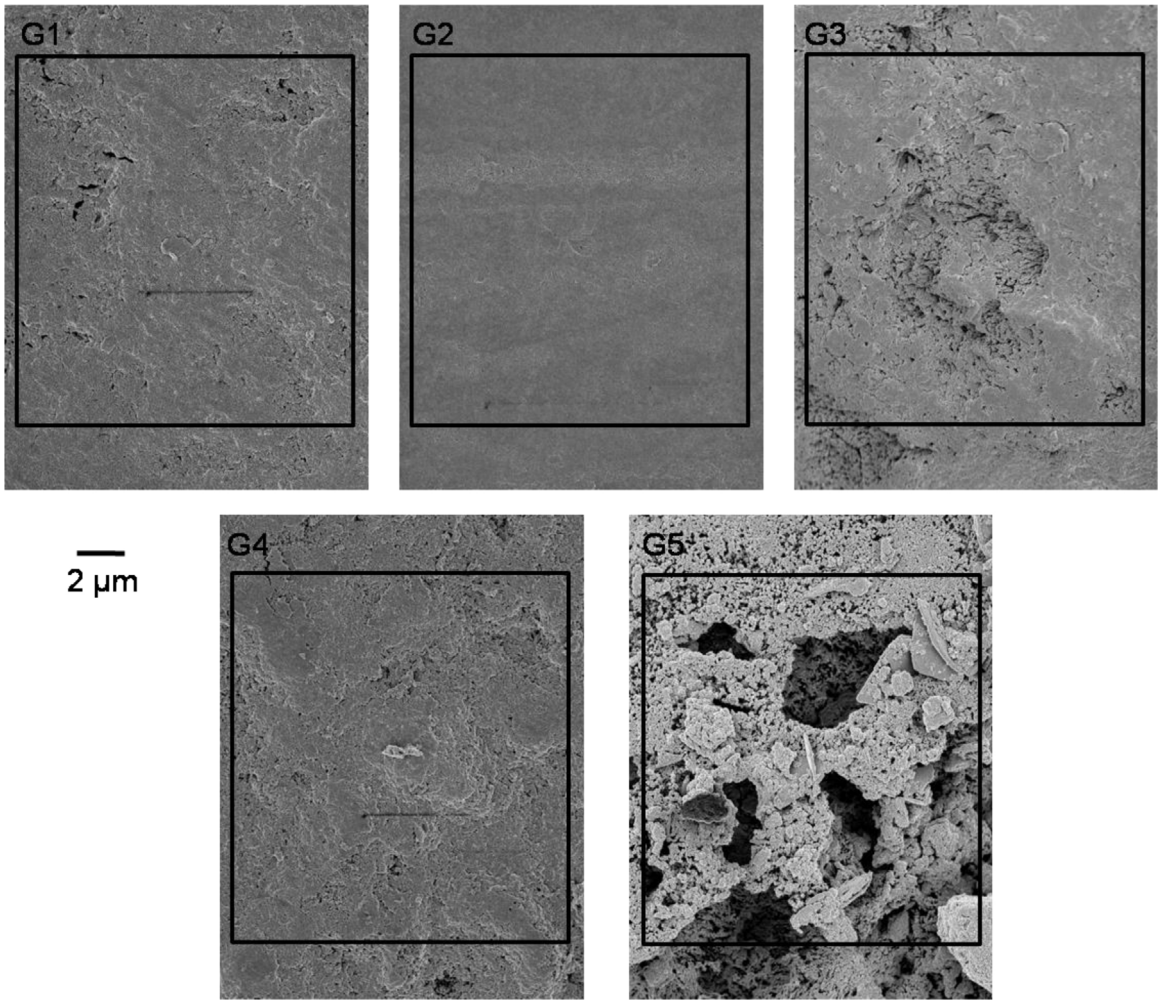

Fig. 1. Secondary electron micrographs corresponding to samples representative of groups G1 (untreated fluorotic molar); G2 (fluorotic molar treated with hydrogen peroxide at 35%.); G3 (fluorotic molar treated with Al_2O_3 + 18% hydrochloric acid (2 min) plus 7 cycles of micro-abrasion (20 s per cycle) and then neutralizer for 30 s); G4 (fluorotic molar treated with hydrochloric acid and micro-abrasion with particles of silicon carbide and neutralizer) and G5 (molar with fluorosis etched with 37% phosphoric acid). All samples selected for this figure bear a TFI score equal to 2.

formation causes a premature mineralization of external enamel and an hipo-mineralized subsuperficial lesion, that microscopically resembles a white or brownish caries lesion. Structural changes in enamel are evident to the naked eye as fine white lines or brown spots on the surface (Peneva, 2008). The type and degree of fluorosis depend on genetic vulnerability and on the development degree of the enamel when the fluorine is ingested (Goldstein and Garber, 1995).

The restoration of natural tooth color can be achieved, in the less severe cases, by applying non-aggressive whitening techniques. At present, whitening techniques are based on the use of bleaching agents such as hydrogen peroxide and carbamide peroxide, and the use of hydrochloric acid or phosphoric acid as erosive elements to enable the micro-abrasion process (Akpata, 2001). If the degree of the stains is mild, whitening is an adequate option; if they are moderate, whitening is applied in first place and then micro-abrasion is performed; in the case of severe stains, the procedure usually applied consists on eroding the stain and then coating the surface with a restorative treatment like veneers.

Micro-abrasion is performed with an abrasive powder of silicon carbide, pumice or alumina. The particles sizes typically range between 10 mm and 100 μm and cause an enamel loss of about 0.2 μm. Since micro-abrasion methods involve a loss of enamel and a generation of chemical reactions, it is important to use techniques that allow surface characteristics to be altered as little as possible. The purpose is to obtain a smooth surface, in order to avoid the deposition of bacterial plaque and of exogenous pigments. It is therefore important to assess the resulting surface roughness of pieces subjected to different treatments.

In this work, the enamel surface of fluorotic dental pieces in vitro was studied by 3D scanning electron microscopy. The surface of teeth under different whitening methods was characterized and compared with untreated pieces. Several functional and amplitude parameters characterizing the surface roughness were computed from the height maps obtained for stereo image pairs, allowing a comparison among the different whitening methods. In order to validate the methodology implemented, sample roughness parameters were checked against the results obtained by conventional confocal laser microscopy.

2. Materials and methods

2.1. Samples

A total number of 25 various molars (mainly third molars) were extracted from adult patients (one piece from each patient) between 30 and 40 years old, for clinical reasons uncorrelated to the fluorosis disease. All patients had similar medical records,

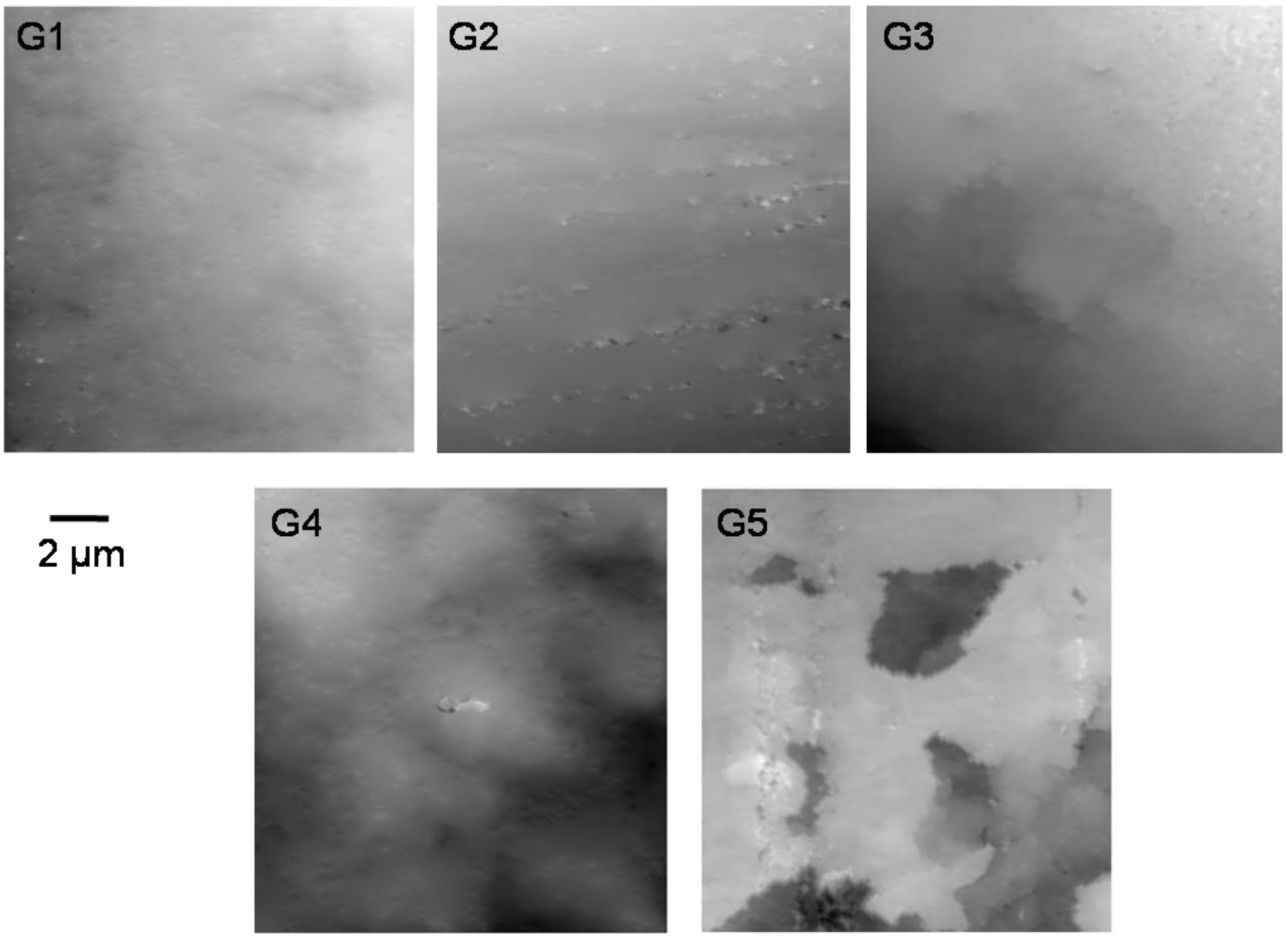

Fig. 2. Height maps obtained from the stereo pairs for the representative samples shown in Fig. 1.

without underlying conditions, and were not under medical treatment; they voluntarily participated knowing they were part of a clinical study. The diagnosis for dental fluorosis was carried out using the Thylstrup and Fejerskov index (TFI), which correlates the clinical appearance of fluorosis with pathological changes in the enamel (Thylstrup and Fejerskov, 1978). This index ranges from zero for a normal tooth to nine for a tooth with very advanced fluorosis; in this last case, the dental piece presents a considerable loss of enamel and changes in the anatomical appearance of the surface (Vieira et al., 2004). In the present study, the TFI was determined by visually examining the dentition, previous to the subsequent extraction. Teeth were first dried for ten seconds using compressed air, and a series of photographs were taken, and then evaluated by two examiners, which determined the corresponding TFI. All the extracted molars had moderate TFI rates, none of them above 4.

The extracted pieces were subjected to an ultrasonic cleaning process, and then classified into five groups according to the treatment applied:

G1: 5 untreated fluorotic teeth.

G2: 5 fluorotic teeth after a 20 min whitening treatment with a 35% hydrogen peroxide agent; pieces were then rinsed with plenty of water.

G3: 5 fluorotic teeth air-abraded with alumina particles; then passed through micro-abrasion with a paste of silicon carbide microparticles and 18% hydrochloric acid and rinsed with plenty of water (up to 10 cycles of 20 s, according to necessity); finally, immersed in a neutralizing solution (30 s).

G4: 5 fluorotic teeth rubbed by hand with a paste of 18% hydrochloric acid and powdered silicon carbide abrasive microparticles and rinsed with plenty of water (up to 10 cycles of 20 s, according to necessity); finally, immersed in a neutralizing solution (30 s).

G5: 5 fluorotic teeth etched with 37% phosphoric acid (10 s) and rinsed with plenty of water.

Treatments for G2, G3 and G4 are usually repeated until the visual perception of the whitening effect is satisfactory. It must be mentioned that the process associated with G5 is not a complete whitening treatment, but only an aggressive initial etching stage intended to the removal of stains.

2.2. Scanning electron microscopy

Secondary electron images were acquired with a Zeiss Σigma FE-SEM (Carl Zeiss Microscopy Ltd., Cambridge). In order to avoid charge accumulation effects and favor the secondary electron emission, the tooth pieces studied were sputtered with a thin gold layer. An energy of 3 keV was found appropriate for the present purposes, secondary electron images being recorded for 5000× magnification by scanning regions of $18 \times 23\ \mu m^2$; lower magnifications allow to survey larger regions, but the spatial resolution worsens, and strong uncertainties are introduced since greater tilt angles are needed (Kang et al., 2012).

The stereo pairs were formed with two tilt angles, 0° and 5°, which were appropriate to characterize these areas at the magnifications set. To this aim, special attention was paid to the allocate the eucentric point, with the aid of the Compucentric Stage® software,

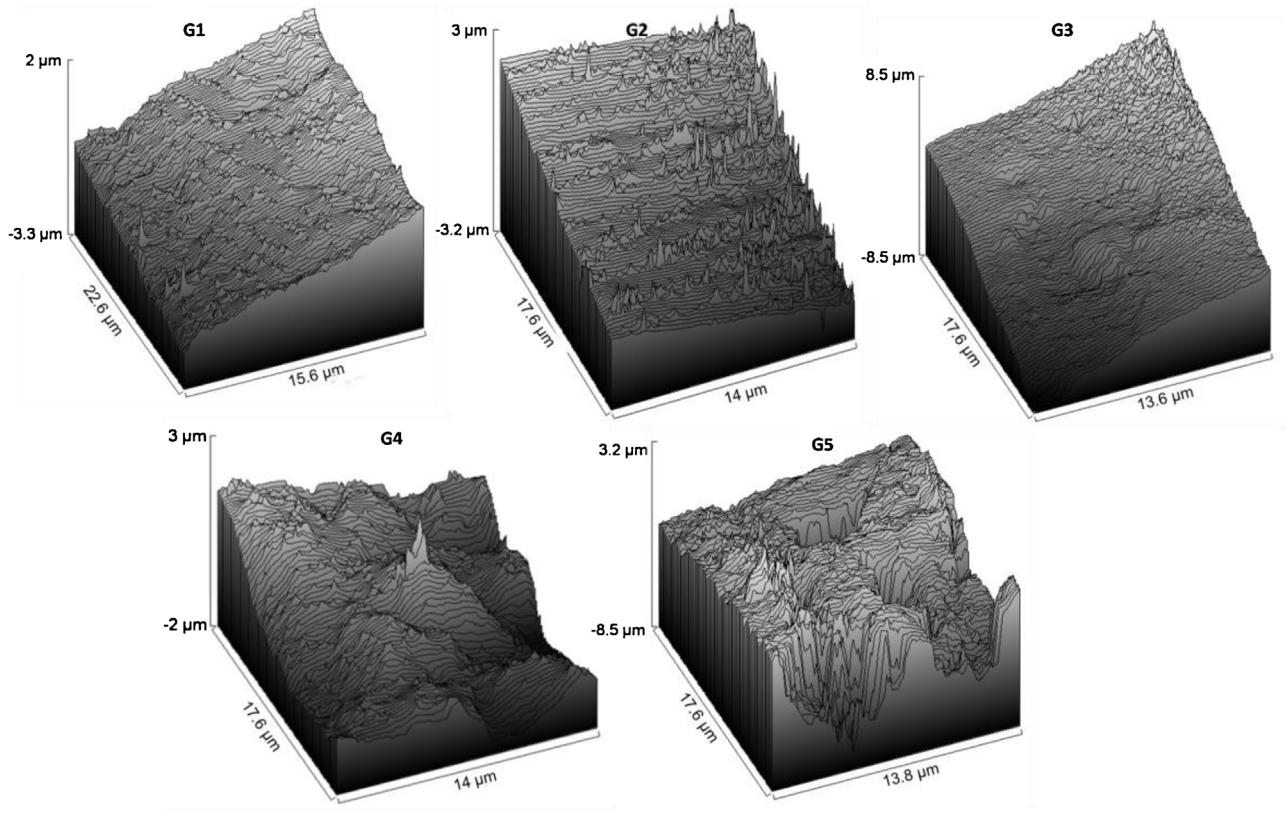

Fig. 3. 3D surface reconstruction obtained from the stereo pairs for the representative samples shown in Fig. 1.

included in the SEM used. In order to transform the stereoscopic pairs in height maps and therefore assess the quantitative roughness parameters the program EZEImage was used (Ponz et al., 2006).

2.3. Estimation of topographic parameters from stereo pairs

The first step to obtain the elevation data is to find the corresponding values of disparity (parallax) between the two images of a stereo pair. The software EZEImage was chosen to perform this correspondence since it allows a fast cross correlation and a two stage dynamic programming: as a first step, a dense disparity map is obtained, and then this auxiliary image is transformed into a dense height map, in which each gray level represents a height value relative to some point in the image (Ponz et al., 2006).

Surface roughness is a texture measure, and is quantified by the vertical deviations of a real surface ($M \times N$ pixels) from its ideal least squares mean plane. There are various parameters to characterize the three dimensional topography of the surface, which are classified according to the property described: amplitude, spatial, hybrid, functional properties, area and volumes. Since it is difficult to interpret and use many of these parameters at once, it is preferable to use a few highly relevant magnitudes (Stout et al., 1993; Dong et al., 1994; Griffiths, 2001). However, the meaning of these specific parameters varies with different applications (Stout and Blunt, 2000). In this work, amplitude and functional parameters are taken into account to characterize the topography for each sample. Amplitude parameters describe variations in height of the structures, and they are determined from the distribution of surface heights relative to the fitted mean plane. The amplitude parameters used in this work are the arithmetic mean deviation of the surface topography (R_a), the root mean square deviation of the surface topography (S_q), the mean value of ten points of maximum and minimum height (S_z), the skewness (S_{sk}) and kurtosis (S_{ku}) of the height distribution, all of them determined from the distribution of surface heights $\eta(i,j)$ relative to the fitted mean plane.

On the other hand, functional parameters characterize the relationship between area and volume. The Abbott–Firestone curve or bearing area curve is the cumulative probability density function of the surface height profile and can be calculated by different methods (Stewart, 1990); this curve divides the surface into three zones: peak zone, core and valley area (Abbott and Firestone, 1933). The functional parameters studied in this work are the surface bearing index (S_{bi}), the core fluid retention index (S_{ci}) and the valley fluid retention index (S_{vi}) (Dong et al., 1994).

3. Results and discussion

Fig. 1 shows secondary electron micrographs acquired at 0° tilt angle and at 5000× magnification, corresponding to samples representative of the five groups studied. The height maps obtained with the software EZEImage (Ponz et al., 2006) after processing the corresponding stereo pairs are also shown in Figs. 2 and 3 as 3D surface plots. These height maps were therefore used to assess the set of amplitude and functional topographic parameters mentioned above. As can be seen, the treatments considered produce a variety of topographic differences, which should be reflected in the characteristic surface parameters. It is important to stress that the magnification chosen for acquiring the SEM images must be kept fix for all samples, in order to take into account topographic features to a similar extent.

The height distribution histograms corresponding to each group are displayed in Fig. 4, along with the resulting bearing area curves. It is clear that the different height distributions allow to identify each group through a visual inspection of these graphs.

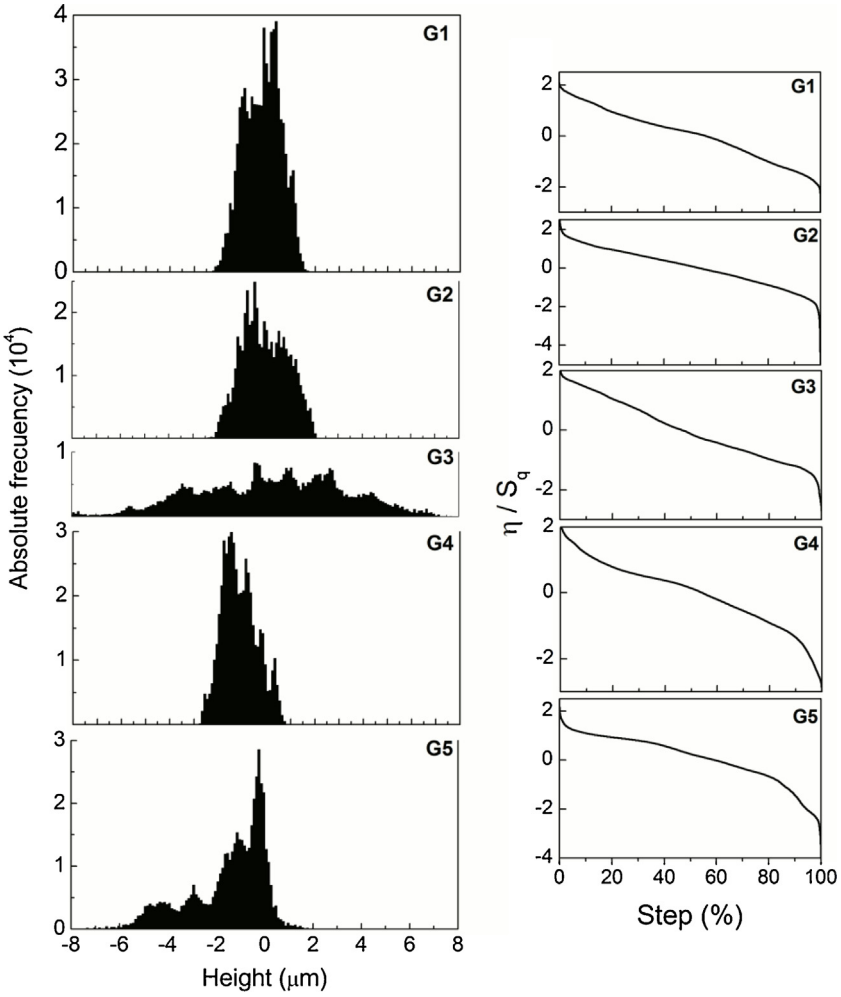

Fig. 4. Height distribution histograms and the resulting bearing area curves for the representative samples shown in Fig. 1.

Table 1
Parameters characterizing the surface roughness of the tooth groups studied.

	G1	G2	G3	G4	G5
S_q (μm)	0.67 ± 0.04	0.310 ± 0.009	1.77 ± 0.09	0.56 ± 0.09	1.6 ± 0.3
R_a (μm)	0.56 ± 0.06	0.260 ± 0.007	1.5 ± 0.1	0.5 ± 0.1	1.3 ± 0.3
S_z (μm)	2.0 ± 0.2	2.2 ± 0.2	4.7 ± 0.2	2.04 ± 0.04	5.5 ± 0.6
S_{ku}	24 ± 18	8 ± 1	4 ± 4	8 ± 1	7 ± 5
S_{sk}	2.4 ± 0.7	−0.7 ± 0.3	−0.2 ± 0.2	0.6 ± 0.3	-1.6 ± 0.6
S_{bi}	0.62 ± 0.7	0.66 ± 0.01	0.61 ± 0.03	0.66 ± 0.01	0.80 ± 0.07
S_{ci}	1.5 ± 0.1	1.39 ± 0.02	1.57 ± 0.07	1.44 ± 0.02	1.01 ± 0.07
S_{vi}	0.08 ± 0.02	0.103 ± 0.004	0.07 ± 0.01	0.12 ± 0.01	0.17 ± 0.01

The results corresponding to the parameters studied for each group of samples are shown in Table 1. In order to provide a quantitative estimate for each parameter, two different regions were considered in each tooth studied; the values displayed in Table 1 arise from the mean values of the parameters for all the sample regions belonging to each of the groups described above, and the uncertainties were estimated as one standard deviation.

It can be seen that the parameters R_a and S_q bear similar trends, which is to be expected since they are both measures of the height dispersion around the fitting plane. Particularly, the lowest values for these parameters correspond to the G2 group (treatment with hydrogen peroxide). Zavala-Alonso et al. (2010) measured the roughness with AFM for third molars with different degrees of fluorosis. The average values for R_a and S_z obtained by them are respectively $(0.093 \pm 0.020)\,\mu m$ and $(1.07 \pm 0.04)\,\mu m$ for control teeth (0 TFI); $(0.19 \pm 0.05)\,\mu m$ and $(2.36 \pm 0.97)\,\mu m$ for fluorotic teeth with TFI between 1 and 3; $(0.25 \pm 0.07)\,\mu m$ and $(2.5 \pm 1.7)\,\mu m$ for pieces with TFI between 4 and 5, and $(0.53 \pm 0.01)\,\mu m$ and $(6.1 \pm 3.4)\,\mu m$ for teeth with TFI between 6 and 9. In this work, R_a and S_z are $(0.56 \pm 0.06)\,\mu m$ and $(2.0 \pm 0.2)\,\mu m$ for fluorotic untreated teeth. According to Zavala-Alonso et al. (2010), this R_a value corresponds to a fluorotic tooth with a high TFI. Instead, our average S_z value would correspond to a tooth with moderate fluorosis, always according to their results; nevertheless, this parameter is very sensitive to pronounced changes in height, which may be related to tooth topographical features, and thus the uncertainties associated to it are quite large (up to 50% in Zavala-Alonso et al., 2010).

The parameter S_{sk} describes the asymmetry of the height distribution. If S_{sk} is zero, heights are symmetrically distributed; if $S_{sk} < 0$,

the surface may mainly bear holes, and if $S_{sk} > 0$, the surface may mainly bear peaks. The high value of S_{sk} for the fluorotic teeth is related to the peaks observed for this group, with scarce voids. The negative value (and large in absolute value) of this parameter for G5 implies a significant presence of voids. Not much more information can be drawn from this parameter, since S_{sk} and S_{ku} bear the largest uncertainties (up to 100%). In particular, the S_{ku} values for all samples are unrelated to the whitening treatments, and present wide variations within a single group of samples. For these reasons, this parameter is not suitable for this application.

The values obtained for the parameter S_{bi} and S_{vi} are practically indistinguishable for all treatments and the untreated tooth, excepting for the G5 group, which must not be considered a complete whitening treatment. By comparing G3 and G4 (which differ in the treatment because of the air abrasion with alumina particles), it can be seen that the alumina particles add certain roughness to the surface that can not be reestablished through a subsequent treatment. This is reflected in the resulting R_a and S_q parameters; however, rubbing with alumina particles appears to slightly influence the S_{sk} and S_{ku} parameters. It is important to stress that this behavior occurs even when the S_q parameters are quite different; the G2 group bears the lowest value, and the resulting S_{ku} and S_{sk} are not so high despite the normalization to S_q in their definition (Dong et al., 1994). In addition, a clear difference is evidenced from the functional parameters for G3 and G4, which implies different retention properties, as a consequence of the combination of air abrasion and micro-abrasion.

The prominent presence of voids in the G5 group (see height image and SEM photo) is mainly reflected in all functional parameters, indicating quite different retention properties resulting for this treatment. The basic principle of acid erosion is to transform the low energy surface into a high energy surface, and to dissolve and demineralize the hydroxyapatite inorganic matrix, creating micropores and microgrooves to improve mechanical retention properties (Torres Gallegos et al., 2012). The use of micro-abrasion to remove the outer fluorotic enamel layers prior to the application of phosphoric acid can improve the enamel surface, providing better retention for subsequent adhesive bonding applications—which is out of the goals pursued in the treatments considered here.

In order to check the validity of the approach faced, a confocal Olympus LEXT OLS4000 3D Laser Measuring Microscope was used for the determination of roughness parameters corresponding to the G5 group. Some of the parameters obtained with the software attached to this instrument are: $S_q = (1.3 \pm 0.2)\,\mu m$, $R_a = (1.0 \pm 0.2)\,\mu m$, $S_z = (12 \pm 2)\,\mu m$, $S_{ku} = (4 \pm 1)$, $S_{sk} = (-1.1 \pm 0.3)$, $S_{ci} = (1.2 \pm 0.2)$, and $S_{vi} = (0.21 \pm 0.03)$. It can be seen that, despite the different spatial resolutions involved, a good agreement is found in most cases, excepting for the parameter S_z; it must however be mentioned that this parameter is strongly dependent on isolated variations in the surface height map, since it takes into account only the most extreme height values.

4. Conclusions

3D scanning electron microscopy proved to be an extremely useful tool to quantify the roughness on the surfaces of the teeth studied. The method used in this survey has advantages such as its low cost, non-destructiveness and rapid implementation; on the other hand optical and laser profiling techniques attain poorer spatial resolution, but sample preparation is much easier. The proposed method was validated by comparing the quantitative roughness parameters obtained with those produced by confocal laser microscopy, a well-established approach for roughness characterization.

The parameters indicative of roughness that vary the most among the different treatments are the values of S_q and R_a. These parameters give an indication of the range of variation in height of the sample surface and were lower in the G2 group treated with hydrogen peroxide, suggesting this method is a convenient whitening alternative, provided that a complete removal of stains is achieved; these results also suggest that hydrogen peroxide may be used as a starting strategy, leaving micro-abrasion for a local strong stain treatment.

The treatment applied to the G5 group (phosphoric acid etching) leaves a rather rough enamel surface, mainly evidenced by the distinctive functional parameters and the corresponding retention properties, which may favor the deposition of bacterial plaque and of exogenous pigments. However, the process associated with G5 is not a complete whitening treatment, but only an aggressive initial etching stage intended to the removal of stains, or a first stage suitable for a subsequent adhesive treatment.

Acknowledgements

This investigation was supported by the Secretaría de Ciencia y Técnica de la Universidad Nacional de Córdoba. The authors thank Tedequim® for providing the employed materials.

References

Abbott, E.J., Firestone, F.A., 1933. Specifying surface quality: a method based on accurate measurement and comparison. Mech. Eng. 55, 569–572.
Akpata, E.S., 2001. Occurrence and management of dental fluorosis. Int. Den. J. 51, 325–333.
Avery, J.K., 1994. Oral Development and Histology, 2nd ed. Thieme, New York.
Bonetto, R.D., Ladaga, J.L., Ponz, E., 2006. Measuring surface topography by scanning electron microscopy II. Analysis of three estimators of surface roughness in second dimension and third dimension. Microsc. Microanal. 12, 178–186.
Bouacha, K., Yallese, M., Mabrouki, T., Rigal, J.-F., 2010. Statistical analysis of surface roughness and cutting forces using response surface methodology in hard turning of AISI 52100 bearing steel with CBN tool. Int. J. Refract. Met. Hard Mater. 28, 349–361.
Choi, S., Park, K.-H., Cheong, Y., Moon, S.W., Park, Y.-G., Park, H.-K., 2012. Potential effects of tooth-brushing on human dentin wear following exposure to acidic soft drinks. J. Microsc. 247, 176–185.
Dong, W.P., Sullivan, P.J., Stout, K.J., 1994. Comprehensive study of parameters for characterising three-dimensional surface topography III: parameters for characterising amplitude and some functional properties. Wear 178, 29–43.
Ferry, V., Sweatlock, L., Pacifici, D., Atwater, H., 2008. Plasmonic nanostructure design for efficient light coupling into solar cells. Nano Lett. 8, 4391––4397.
Ficker, T., Martišek, D., Jennings, H., 2010. Roughness of fracture surfaces and compressive strength of hydrated cement pastes. Cem. Concr. Res. 40, 947–955.
Gittens, R., McLachlan, T., Olivares-Navarrete, R., Cai, Ye, Berner, S., Tannenbaum, R., Schwartz, Z., Sandhage, K., Boyan, B., 2011. The effects of combined micron/submicron-scale surface roughness and nanoscale features on cell proliferation and differentiation. Biomaterials 32, 3395–3403.
Goldstein, R.E., Garber, D.A., 1995. Complete Dental Bleaching. Quintessence Publishing, IL, ISBN-10: 0867152907 ISBN-13: 978-0867152906.
Griffiths, B., 2001. Manufacturing Surface Technology: Surface Integrity & Functional Performance. Penton Press, London.
Harrison, A.P., Wong, C.M., Joseph, D., 2011. Virtual reflected-light microscopy. J. Microsc. 244, 293–304.
Kang, K.W., Pereda, M.D., Canafoglia, M.E., Bilmes, P., Llorente, C., Bonetto, R.D., 2012. Uncertainty studies of topographical measurements on steel surface corrosion by 3D scanning electron microscopy. Micron 43, 387–395.
Kim, K.W., 2015. Three-dimensional surface reconstruction and in situ site-specific cutting of the teliospores of *Puccina miscanthi* causing leaf rust of the biomass plant *Miscanthus sinesis*. Micron 73, 15–20.
Kohn, W.G., Maas, W.R., Malvitz, D.M., Presson, S.M., Shaddix, K.K., 2001. Recommendations for using fluoride to prevent and control dental caries in the United States. Morb. Mortal. Wkly. Rep. 50, 1–42.
Mohr, D., Wray, G., 1976. Stereoscopy techniques for the electron microscope. Ultramicroscopy 1, 181–186.
Peneva, M., 2008. Treatment of dental fluorosis. In: Peytchinski, G.I. (Ed.), J. IMAB Ann. Proc. 14, 71–74.
Piazzesi, G., 1973. Photogrammetry with the scanning electron microscope. J. Phys. E: Sci. Instrum. 6, 392–396.
Ponz, E., Ladaga, J.L., Bonetto, R.D., 2006. Measuring surface topography with scanning electron microscopy. I. EZEImage: a program to obtain 3D surface data. Microsc. Microanal. 12, 170–177.

Reimer, L., 1998. Scanning electron microscopy physics of image formation and microanalysis. Springer Ser. Opt. Science, vol. 45., 2nd. ed. Springer-Verlag, Berlin–Heidelberg.
Richards, R.G., Wieland, M., Textor, M., 2000. Advantages of stereo imaging of metallic surfaces with low voltage backscattered electrons in a field emission scanning electron microscope. J. Microsc. 199, 115–123.
Schubert, M., Gleichmann, A., Hemmleb, M., Albertz, J., Köhler, J.M., 1996. Determination of the height of a microstructure sample by a SEM with a conventional and a digital photogrammetric method. Ultramicroscopy 63, 57–64.
Stewart, M., 1990. A new approach to the use of bearing area curve. In: International Honing Technologies and Applications: Conferenc. FC90-229, Dearborn, Mich.: Society of Manufacturing Engineers.
Stout, K., Blunt, L., 2000. Three-Dimensional Surface Topography, 2nd ed. Penton Press, London.
Stout, K.J., Sullivan, P.J., Dong, W.P., Mainsah, E., Luo, N., Mathia, T., Zahouani, H., 1993. The development of methods for the characterization of roughness in three dimensions. In: Commission of European Communities, Directorate General XII, Science, Research and Development, Report EUR 15178. ECSCEECEAEC, Brussels–Luxembourg.
Tafti, A.P., Kirkpatrick, A.B., Alavi, Z., Owen, H.A., Yu, Z., 2015. Recent advances in 3D SEM surface reconstruction. Micron 78, 54–66.
Thylstrup, A., Fejerskov, O., 1978. Clinical appearance of dental fluorosis in permanent teeth in relation to histologic changes. Community Dent. Oral Epidemiol. 6, 315–328.
Torres Gallegos, I., Zavala-Alonso, V., Patiño-Marin, N., Martinez-Castañon, G.A., Anusavice, K., Loyola-Rodriguez, J.P., 2012. Enamel roughness and depth profile after phosphoric acid etching of healthy and fluorotic enamel. Aust. Dent. J. 57, 151–156.
Vieira, A., Hancock, R., Limeback, H., Maia, R., Grynpas, M., 2004. Is fluoride concentration in dentin and enamel a good indicator of dental fluorosis? J. Dent. Res. 83, 76–80.
Zavala-Alonso, V., Martínez-Castanon, G., Patiño-Marín, N., Terrones, H., Anusavice, K., Loyola-Rodríguez, J., 2010. Characterization of healthy and fluorotic enamel by atomic force microscopy. Microsc. Microanal. 16, 531–536.